Measurement of the double-β decay half-life of 150Nd and search for neutrinoless decay modes with the NEMO-3 detector

J. Argyriades, R. Arnold, C. Augier, J. Baker, A.S. Barabash, A. Basharina-Freshville, M. Bongrand, G. Broudin, V. Brudanin, A.J. Caffrey, et al.

Measurement of the Double Beta Decay Half-life of ^{150}Nd and Search for Neutrinoless Decay Modes with the NEMO-3 Detector

J. Argyriades[1], R. Arnold[2], C. Augier[1], J. Baker[3], A.S. Barabash[4], A. Basharina-Freshville[5], M. Bongrand[1], G. Broudin[6,7], V. Brudanin[8], A.J. Caffrey[3], E. Chauveau[6,7], Z. Daraktchieva[5], D. Durand[9], V. Egorov[8], N. Fatemi-Ghomi[10], R. Flack[5], Ph. Hubert[6,7], J. Jerie[13], S. Jullian[1], M. Kauer[5], S. King[5], A. Klimenko[8], O. Kochetov[8], S.I. Konovalov[4], V. Kovalenko[8], D. Lalanne[1], T. Lamhamdi[11], K. Lang[12], Y. Lemière[9], C. Longuemare[9], G. Lutter[6,7], Ch. Marquet[6,7], J. Martin-Albo[14], F. Mauger[9], A. Nachab[6,7], I. Nasteva[10], I. Nemchenok[8], F. Nova[15], P. Novella[14], H. Ohsumi[16], R.B. Pahlka[12], F. Perrot[6,7], F. Piquemal[6,7], J.L. Reyss[17], J.S. Ricol[6,7], R. Saakyan[5], X. Sarazin[1], L. Simard[1], F. Šimkovic[18], Yu. Shitov[8], A. Smolnikov[8], S. Snow[10], S. Söldner-Rembold[10], I. Štekl[13], J. Suhonen[19], C.S. Sutton[20], G. Szklarz[1], J. Thomas[5], V. Timkin[8], V. Tretyak[8], V. Umatov[4], L. Vála[13], I. Vanyushin[4], V. Vasiliev[5], V. Vorobel[21], and Ts. Vylov[8]

(The NEMO Collaboration)

[1]*LAL, Université Paris-Sud 11, CNRS/IN2P3, Orsay, France*
[2]*IPHC, Université de Strasbourg, CNRS/IN2P3, F-67037 Strasbourg, France*
[3]*INL, Idaho Falls, Idaho 83415, USA*
[4]*Institute of Theoretical and Experimental Physics, 117259 Moscow, Russia*
[5]*University College London, WC1E 6BT London, United Kingdom*
[6]*Université de Bordeaux, Centre d'Etudes Nucléaires de Bordeaux Gradignan, UMR 5797, F-33175 Gradignan, France*
[7]*CNRS/IN2P3, Centre d'Etudes Nucléaires de Bordeaux Gradignan, UMR 5797, F-33175 Gradignan, France*
[8]*Joint Institute for Nuclear Research, 141980 Dubna, Russia*
[9]*LPC Caen, ENSICAEN, Université de Caen, Caen, France*
[10]*University of Manchester, M13 9PL Manchester, United Kingdom*
[11]*USMBA, Fes, Morocco*
[12]*University of Texas at Austin, Austin, Texas 78712-0264, USA*
[13]*IEAP, Czech Technical University in Prague, CZ-12800 Prague, Czech Republic*
[14]*IFIC, CSIC - Universidad de Valencia, Valencia, Spain*
[15]*Universitat Autònoma de Barcelona, Spain*
[16]*Saga University, Saga 840-8502, Japan*
[17]*LSCE, CNRS, F-91190 Gif-sur-Yvette, France*
[18]*FMFI, Comenius University, SK-842 48 Bratislava, Slovakia*
[19]*Jyväskylä University, 40351 Jyväskylä, Finland*
[20]*MHC, South Hadley, Massachusetts 01075, USA and*
[21]*Charles University, Prague, Czech Republic*
(Dated: October 29, 2018)

The half-life for double beta decay of ^{150}Nd has been measured by the NEMO-3 experiment at the Modane Underground Laboratory. Using 924.7 days of data recorded with 36.55 g of ^{150}Nd the half-life for $2\nu\beta\beta$ decay is measured to be $T_{1/2}^{2\nu} = (9.11_{-0.22}^{+0.25}(\text{stat.}) \pm 0.63\,(\text{syst.})) \times 10^{18}$ years. The observed limit on the half-life for neutrinoless double beta decay is found to be $T_{1/2}^{0\nu} > 1.8 \times 10^{22}$ years at 90% Confidence Level. This translates into a limit on the effective Majorana neutrino mass of $\langle m_\nu \rangle < 4.0 - 6.3$ eV if the nuclear deformation is taken into account. We also set limits on models involving Majoron emission, right-handed currents and transitions to excited states.

PACS numbers: 14.60.Pq, 23.40.-s

Experiments studying atmospheric, solar, reactor and accelerator neutrinos have established the existence of neutrino oscillations as a direct evidence for a non-zero neutrino mass. These experiments, however, cannot distinguish between Dirac or Majorana neutrinos. They also provide no information on the absolute neutrino mass scale, since oscillations experiments measure the square of the mass difference between neutrino states. The half-life of neutrinoless double beta decay ($0\nu\beta\beta$) is inversely proportional to the effective Majorana neutrino mass squared, $\langle m_\nu \rangle^2$. Observation of this process would therefore directly constrain the neutrino mass scale and would be unambiguous evidence for the Majorana nature of neutrinos. The $0\nu\beta\beta$ process also violates lepton number and is therefore a direct probe for physics beyond the standard model of particle physics.

The search for neutrinoless double beta decay of neodymium-150 (^{150}Nd) using the NEMO-3 detector is of special interest since ^{150}Nd is a candidate isotope for SuperNEMO [1], a next generation double beta decay experiment based on the NEMO-3 concept, and the SNO++ experiment at SNOLAB [2]. Its main advan-

tages are the high $Q_{\beta\beta}$ value for double beta decay, $Q_{\beta\beta}$ = 3.368 MeV, which lies above the typical energies for many background sources, and the large phase space factor. The $2\nu\beta\beta$ half-life of ^{150}Nd has previously been measured using a Time Projection Chamber [3, 4].

The NEMO-3 experiment has been taking data since 2003 in the Modane Underground Laboratory (LSM) located in the Fréjus tunnel at a depth of 4800 m water equivalent. The detector has a cylindrical shape with 20 sectors that contain different isotopes in the form of thin foils with a total surface of about 20 m² [5]. In addition to ~7 kg of ^{100}Mo and ~1 kg of ^{82}Se, the detector contains smaller amounts of other isotopes. The neodymium source foil is composed of Nd_2O_3 with an enrichment of (91 ± 0.5)%, corresponding to a ^{150}Nd mass of 36.55 ± 0.10 g. On each side of the foils is a ~50 cm wide tracking volume comprising a total of 6180 drift cells operated in Geiger mode with helium as drift gas. A 25 Gauss magnetic field created by a solenoid provides charge identification. The calorimeter consists of 1940 plastic scintillators coupled to low radioactivity photomultipliers. For 1 MeV electrons the energy resolution (FWHM) ranges from 14.1% to 17.7% and the timing resolution is 250 ps. A cylindrical coordinate system (r, z, φ) is used with the z axis pointing upwards.

The data used in this Letter have been recorded between February 2003 and December 2006, corresponding to 924.7 days of data taking. Signal and background events are generated with the GENBB generator and simulated using a GEANT-based simulation [6] of the detector. All Monte Carlo events are processed by the same reconstruction programs as the data. A detailed description of the analysis can be found in [7].

The $2\nu\beta\beta$ events are expected to have two electrons in the final state and they are therefore selected by requiring two tracks with a curvature consistent with a negative charge. Each track has to be matched to a separate energy deposit in the calorimeter greater than 0.2 MeV. The z component of the distance between the intersections of each track with the plane of the foil should be less than 4 cm and the transverse component less than 2 cm. Both tracks must originate from the first layer of the Geiger cells. The scintillator measurement of the time-of-flight (TOF) for both electron candidates must be consistent with the hypothesis that the event originates from the source foil. After this selection 2789 events remain.

The background sources are divided into two categories, depending on their origin [8]. Background events originating from the radioactive impurities in the source foils are called internal background. β emitters can produce $\beta\beta$-like events through three mechanisms: (i) β decay accompanied by electron conversion; (ii) Møller scattering of a β decay electron, and (iii) β decay to an excited state followed by Compton scattering of the de-excitation photon. Another internal background source is ^{207}Bi, most likely present due to a contamination of the

^{150}Nd source foil during production. This isotope decays to excited ^{207}Pb through electron capture and ^{207}Pb subsequently emits two electrons via electron conversion.

The second source of background is called external and is caused by electrons or photons anywhere outside the source foils. The main source of external background is radon. Radon decays to ^{214}Bi via two α decays and one β^- decay. The decay of ^{214}Bi to ^{214}Po is generally accompanied by one electron and several photons, which can mimic a $\beta\beta$ event through conversions. A radon purification facility was installed about half-way through the data taking period presented in this Letter. This reduces the radon induced background for this analysis by about a factor of six. Other external background contributions are found to be small.

The background activities are determined by measuring control decay channels that are independent of the signal topology using a full MC simulation of the background processes and the detector. A summary of the measured background activities are given in Table I.

In the $e\gamma$ channel, ^{207}Pb from the ^{207}Bi decays via the emission of an electron and a photon from the strongly-converted energy transition in excited ^{207}Pb. ^{152}Eu decays into excited ^{152}Gd through β decay which de-excites into the ground state via photon emission. The $e\gamma$ events are selected by requiring that exactly one negatively charged particle with a track length greater than 50 cm is found in the sector containing the ^{150}Nd foil. The track must be associated with an isolated scintillator hit with energy greater than 0.2 MeV. It must originate from the ^{150}Nd foil and must have a hit in the first layer of the Geiger cells. The scintillator measurement of the time-of-flight of the electron candidates has to be consistent with the hypothesis that the decay occurred in the source foil. The photon is identified by requiring that there is a second scintillator hit with no associated track and with energy greater than 0.2 MeV. The energy sum of the all other clusters not associated to the electron or the photon must be less than 0.15 MeV. The opening angle between the electron and the photon is required to be $\cos\vartheta < 0.9$.

To obtain the background normalisation for ^{207}Bi and ^{152}Eu, the normalization of these background contributions is fitted to spectra of the electron energies, E_e, and the photon energies, E_γ, shown in Figure 1. The contributions from other background sources are fixed in the fit. The ^{228}Ac contribution is taken from the ^{208}Tl component in the high energy tail of the E_γ distribution, since ^{208}Tl originates from ^{228}Ac decays. The ^{212}Bi component is normalised with respect to the measurement of its decay product ^{208}Tl. The external, the radon induced, ^{214}Bi and ^{214}Pb backgrounds are set to their independently measured values.

The isotopes ^{234m}Pa and ^{40}K undergo β decay. Their activities are therefore measured with single electron events. The same selection for the electron is applied as in the $e\gamma$ channel, apart from an additional require-
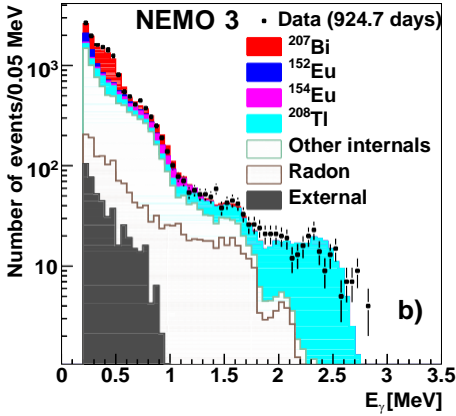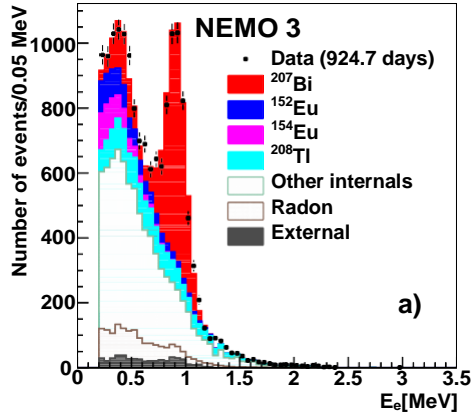
FIG. 1: (color online) Energy distributions of the a) electrons and b) photons in $e\gamma$ events. The data with statistical uncertainties are compared to the sum of the expected background.

FIG. 2: (color online) Distribution of the electron energy in single electron events. The data are compared to the sum of the expected background.

Background	A (mBq/kg)	N_{bg}	N_{bg} for $E_{\text{sum}} > 2.5$ MeV
^{152}Eu	54 ± 6	19 ± 1	0
^{154}Eu	22 ± 2	9 ± 1	0
^{208}Tl	10 ± 2	46 ± 4	3.5 ± 0.9
^{228}Ac	27.8 ± 5.6	52 ± 5	0
^{212}Bi	27.8 ± 5.6	32 ± 4	0
^{207}Bi	231 ± 10	138 ± 6	0
^{214}Bi	3.3 ± 0.8	13 ± 3	0.6 ± 0.2
^{214}Pb	3.3 ± 0.8	6 ± 1	0
^{40}K	213 ± 10	66 ± 6	0
^{234m}Pa	47 ± 2	143 ± 6	0
External and radon induced		53 ± 11	4.8 ± 0.8
^{48}Ca, ^{96}Zr, ^{100}Mo		168 ± 19	0.12 ± 0.02
sum		746 ± 30	9.0 ± 1.2
data		2789	29

TABLE I: Summary of the measured background activities, the expected number of background events and the observed number of events for the selected data set and in the high energy region, $E_{\text{sum}} > 2.5$ MeV.

ment $E_e > 0.5$ MeV. The ^{234m}Pa and ^{40}K contributions are obtained from a fit of the normalization to the E_e distributions. The external background is set to the values obtained from independent measurements. The ^{207}Bi component has been measured in the $e\gamma$ channel. The E_e distribution with the fitted ^{234m}Pa and ^{40}K contributions is shown in Figure 2. The distribution of the event vertices for the single electron events, calculated as the electron track's intersection with the source foil, shows small regions of high activity consistent with ^{234m}Pa contamination which are removed from the analysis. The activities given in Table I. are measured after the removal of these regions.

Due to the resolution of the tracking detector, events from neighboring source foils (^{48}Ca, ^{96}Zr, ^{100}Mo) can be reconstructed as originating from the ^{150}Nd foil. The total number of background events from neighboring foils is estimated to be 126 ± 12 from MC simulations, where the uncertainty is dominated by the uncertainty on the half-life of these isotopes.

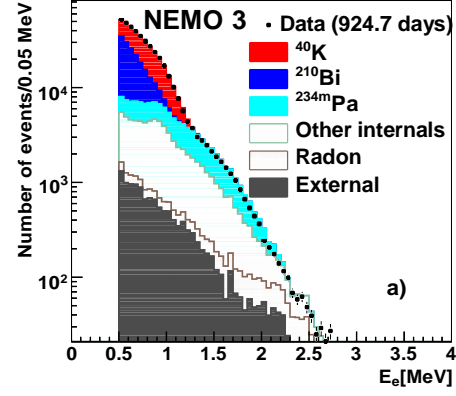The distributions of the energy sum of the two elec-

trons and the opening angle between them are shown in Figure 3. The data are in good agreement with the sum of the background and the $2\nu\beta\beta$ signal distributions. We therefore use the data sample to measure the $2\nu\beta\beta$ half-life, $T^{2\nu}_{1/2}$ of ^{150}Nd. The efficiency of the $2\nu\beta\beta$ event selection is 7.2%. After background subtraction we obtain

$$T^{2\nu}_{1/2} = (9.11^{+0.25}_{-0.22}(\text{stat.}) \pm 0.63 \ (\text{syst.})) \times 10^{18} \ \text{y} . \quad (1)$$

The systematic uncertainty on the sum of the internal and external background is 4.3% which translates into an uncertainty on the $2\nu\beta\beta$ half-life of 1.6%. This includes the uncertainty from the background fits and from the measurement of the activity of ^{208}Tl using two different
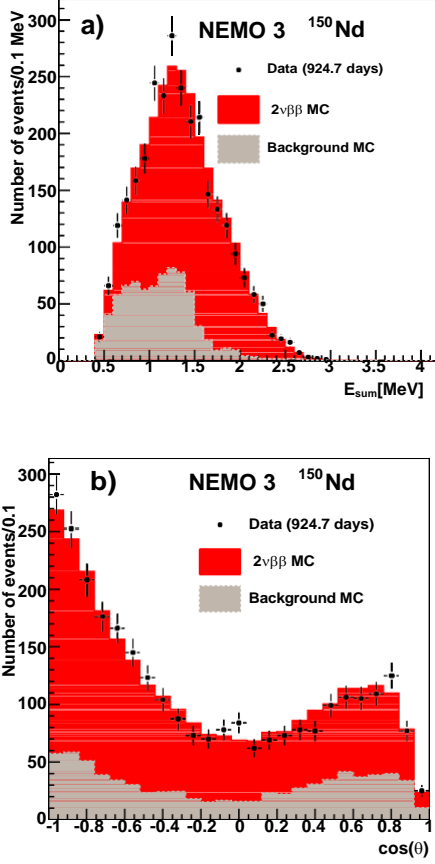
FIG. 3: (color online) Distributions of a) the energy sum of the two electrons, E_{sum}, and b) the angle between the two electrons, cos θ, for data compared to the sum of the background and $2\nu\beta\beta$ signal expectations.

populated using Poisson simulations of the two hypotheses. Systematic uncertainties are treated as uncertainties on the expected numbers of events and are folded into the signal and background expectations via a Gaussian distribution. Correlations between systematic uncertainties are taken into account. The value of the confidence level, CL_s, is defined as $CL_s = CL_{s+b}/CL_b$, where CL_{s+b} and CL_b are the confidence levels in the signal-plus-background and background only hypotheses, respectively. The limits are calculated by scaling the signal until $1 - CL_s$ reaches 0.9.
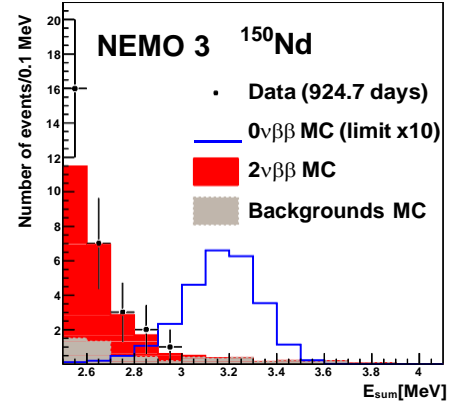

FIG. 4: (color online) Distribution of the energy sum of the two electrons, E_{sum}, for $E_{sum} > 2.5$ MeV. The data are compared to the total background, consisting of internal and external background and the $2\nu\beta\beta$ expectation. A MC simulation of a $0\nu\beta\beta$ signal with a half-life of 1.8×10^{21} years, corresponding to ten times the number of events expected for the observed 90% C.L. limit, is also shown.

decay channels. The uncertainty on the tracking efficiency is 5.7%. Varying the TOF requirement leads to a 1% uncertainty. An uncertainty of 3% is due to the uncertainty on the position of the ^{150}Nd foil in the detector. The uncertainty on the energy measurement was studied by smearing the individual electron energies by 2% which yields a systematic uncertainty of 1.5% on the $2\nu\beta\beta$ half-life.

Since no significant excess is observed in the E_{sum} distribution, a limit is set on the half-life for neutrinoless double beta decay, $T_{1/2}^{0\nu}$, using the CL_s method [9]. Only the shapes and not the normalization of the full E_{sum} distribution are used to discriminate signal and $2\nu\beta\beta$ background. The normalization of the E_{sum} distribution for the other backgrounds is fixed to the value given in Table I. All limits in this Letter are calculated by utilizing a likelihood-fitter [10] that uses a log-likelihood ratio (LLR) test statistic method. Two hypotheses are defined, the signal-plus-background hypothesis and the background-only hypothesis. The LLR distributions are

The total efficiency for $0\nu\beta\beta$ events after applying all selections is (19±1)%. The uncertainties on the efficiency of the signal and the background are assumed to be fully correlated. The E_{sum} distribution for $E_{sum} > 2.5$ MeV is shown in Figure 4 for data compared to the total background, which consists of internal and external background and the $2\nu\beta\beta$ expectation. A MC simulation of a $0\nu\beta\beta$ signal is also shown. Signal and background are well separated, demonstrating the advantages of using ^{150}Nd for future $0\nu\beta\beta$ searches. The observed limit on the half-life is $T_{1/2}^{0\nu} > 1.8 \times 10^{22}$ years at 90% Confidence Level (CL). It is consistent with the median expected limit.

This limit on the half-life is converted into a limit on the effective Majorana neutrino mass, $\langle m_\nu \rangle$, using nuclear matrix elements (NME). In the currently available QRPA-like calculations spherical symmetry of the nucleus has been assumed. If the upper and lower limits on the calculated NME, which also include the uncertainties in the weak coupling constant g_A, are taken into account [11], the experimental lower limit on the half-life

of ^{150}Nd translates into a limit $\langle m_\nu \rangle < 1.5 - 2.5$ eV.

Taking into account the nuclear deformation will modify this conclusion. The suppression of the NME for ^{150}Nd has been estimated to be a factor 2.7 in the case of nuclear deformations derived from laboratory moments [12]. This increases the upper limit to $\langle m_\nu \rangle <$ 4.0 − 6.8 eV which is consistent with the limit derived using the NME of a pseudo SU(3) model [13] and the PHFB model [14], which also include the effect of nuclear deformation. Further progress in the calculation of the NME for 0$\nu\beta\beta$ decay of ^{150}Nd is therefore urgently required.

Neutrinoless double beta decay can also proceed through the emission of one or two Majorons (χ^0) [15]. These decays are characterized by the spectral index n which leads to a modification of the energy sum distribution by a factor $(Q_{\beta\beta} - E_{sum})^n$. We consider models with $n = 1, 3, 7$ [15] and $n = 2$ [16]. Limits on $n = 3, 7$ models are less sensitive than $n = 1, 2$ since the shape of the E_{sum} distribution is similar to the one for 2$\nu\beta\beta$ decay ($n = 5$). The CL_s method is applied to the E_{sum} distribution in the same way as described previously. Since the normalisation of the 2$\nu\beta\beta$ background can not be independently determined, it is left unconstrained in the fit determining the limits.

We also set limits for 0$\nu\beta\beta$ processes involving right-handed currents (V+A). In addition, the 0$\nu\beta\beta$ decay can also proceed through various excited states (0^+ or 2^+_1). Limits on all these modes of neutrinoless double beta decay are shown in Table II. They either improve previously published limits [4, 17] significantly or represent the first limits for this isotope ($n = 2, 3, 7$). The limit on $n = 1$ Majoron emission can be be translated into a limit on the neutrino-Majoron coupling of $g_{ee} <$ $(0.64 - 1.05) \times 10^{-4}$ without and $g_{ee} < (1.7 - 3.0) \times 10^{-4}$ with nuclear deformation. These limits are comparable with the limits obtained for ^{82}Se and ^{100}Mo with about 9 and 70 times the exposure, defined by isotope mass times observation time [18].

	0$\nu\beta\beta$				Majorons			
	0^+_{gs} ($\langle m_\nu \rangle$)	0^+_{gs} (V+A)	2^+_1	0^+_1	$n=1$	$n=2$	$n=3$	$n=7$
limit	18.0	10.7	2.4	0.24	1.52	0.54	0.22	0.047

TABLE II: 90% C.L. limits on the half-life, $T_{1/2}$, in units of 10^{21} y, for different modes of neutrinoless double beta decay.

In summary, we have presented the most precise mea-surement of the half-life of double beta decay of ^{150}Nd to date, yielding a value of $T^{2\nu}_{1/2} = (9.11^{+0.25}_{-0.22}(\text{stat.}) \pm 0.63$ (syst.)) $\times 10^{18}$ years. This value is slightly more than two standard deviations higher than the previously measured value $T^{2\nu}_{1/2} = (6.75^{+0.37}_{-0.42}(\text{stat.}) \pm 0.68$ (syst.)) $\times 10^{18}$ years [4]. We have significantly improved limits on the half-life of different modes of neutrinoless double beta decay for ^{150}Nd and we have provided the first limits for several Majoron models using ^{150}Nd. Our measurements demonstrate that ^{150}Nd is an excellent candidate isotope for future double beta decay experiments.

[1] F. Piquemal, Phys. Atom. Nucl. 69, 2096 (2006).
[2] K. Zuber, AIP Conf. Proc. 942, 101 (2007).
[3] V. Artemiev et al., Phys. Lett. B 345, 564 (1995).
[4] A. De Silva et al., Phys. Rev. C 56, 2451 (1997).
[5] R. Arnold et al., Nucl. Instrum. Methods A 536, 79 (2005).
[6] R. Brun and F. Carminati, CERN Program Library Long Writeup W5013, 1993 (unpublished).
[7] N. Fatemi-Ghomi, PhD Thesis, University of Manchester, arXiv:0905.0822 (2009).
[8] J. Argyriades et al., arXiv:0903:2277, submitted to Nucl. Instr. Method A.
[9] T. Junk, Nucl. Instrum. Methods A 434, 435 (1999).
[10] W. Fisher, FERMILAB-TM-2386-E (2007).
[11] V.A. Rodin et al., Nucl. Phys. A 766, 107 (2006) and erratum 793, 213 (2007).
[12] F. Šimkovic, AIP Conf. Proc. 942, 77 (2007).
[13] J.G. Hirsch, O. Castanos and P.O. Hess, Nucl. Phys. A 582, 124 (1995).
[14] K. Chaturvedi et al., arXiv:0805.4073 [nucl-th].
[15] P. Bamert, C.P. Burgess and R.N. Mohapatra, Nucl. Phys. B 449, 25 (1995).
[16] R.N. Mohapatra, A. Perez-Lorenzana and C.A. De S. Pires, Phys. Lett. B. 491, 143 (2000).
[17] A.A. Klimenko, A.A. Pomansky and A.A. Smolnikov, Nucl. Instr. Meth.17, 445 (1986); C. Arpesella et al., Nucl. Phys. B. 70, 249 (1999); A.A. Klimenko et al., Czech. J. Phys. 52, 589 (2002).
[18] R. Arnold et al., Nucl. Phys. A765, 483 (2006).